Mid-Infrared Chemical Sensors Utilizing Plasma-Deposited Fluorocarbon Membranes

ARTICLE *in* ANALYTICAL CHEMISTRY · JANUARY 2008

Impact Factor: 5.64 · DOI: 10.1021/ac070832g · Source: PubMed

Anal. Chem. **2007,** *79,* 9566−9571

Technical Notes

Mid-Infrared Chemical Sensors Utilizing Plasma-Deposited Fluorocarbon Membranes

Gary T. Dobbs,[†] Balamurali Balu,[‡] Christina Young,[†] Christine Kranz,[†] Dennis W. Hess,[‡] and Boris Mizaikoff*,[†]

School of Chemistry and Biochemistry, Georgia Institute of Technology, 901 Atlantic Drive NW, Atlanta, Georgia 30332-0400, and School of Chemical and Biomolecular Engineering, Georgia Institute of Technology, 311 Ferst Drive NW, Atlanta, Georgia 30332-0100

In this study, plasma-polymerized films are evaluated as enrichment membranes deposited at the surface of mid-infrared transparent waveguides for liquid-phase chemical sensing utilizing evanescent field absorption spectroscopy. Fluorocarbon films were deposited onto zinc selenide (ZnSe) waveguides from plasma-polymerized pentafluoroethane (CF_3CHF_2) vapor. Excellent optical transmission of ZnSe waveguides after plasma deposition confirms compatibility of the infrared transparent substrate with this low-temperature, solvent-free film deposition process. The liquid-phase enrichment characteristics for plasma membranes were investigated via evanescent field absorption spectroscopy of a model analyte (tetrachloroethylene); the limits of detection were below 300 ppb (v/v) in water. Plasma-polymerized films are known for their excellent mechanical and chemical stability, while offering tunable chemical and physical characteristics during the deposition process. Future application of this coating strategy for depositing robust enrichment membranes with tunable batch production capability imparts an attractive route toward application-oriented development of next-generation mid-infrared chemical sensors applicable in harsh environments.

Optical chemical sensors utilizing infrared attenuated total reflection (IR-ATR) induced evanescent field absorption spectroscopy provide the capability of evaluating volatile organic compounds (VOCs) in aqueous environments with either planar waveguides or fiber-optic transducers.[1−16] IR-ATR sensors tailored to detect and monitor trace-level VOCs in aqueous matrices invoke a thin (0.3−3 μm) enrichment membrane that is coated onto the waveguide/transducer substrate. The specific membrane, usually comprised of a polymer or sol−gel, is targeted for extraction and enhancement of the analyte signal, which is generated by molecule-specific absorption of light via interaction with the evanescent field.[17,18] IR-ATR spectroscopy provides a sensitive yet simple instrumental scheme for environmental and industrial monitoring applications. Utilization of membrane-coated IR-ATR waveguides enables ppb (v/v) detection limits for a wide variety of VOCs with low susceptibility to temperature, turbidity, salinity, and humic acids, which are commonly encountered during direct analysis of aqueous environments.[3,5,8,10,11]

In general, two classes of enrichment membranes have to date been utilized for liquid-phase IR-ATR sensors: polymer membranes[1,4,19] and sol−gel materials.[20−23] Polymer membranes are usually reconstituted from organic solutions of a dissolved polymer

* To whom correspondence should be addressed. Phone: 404-894-4430. Fax: 404-385-6447. E-mail: boris.mizaikoff@chemistry.gatech.edu.

[†] School of Chemistry and Biochemistry.

[‡] School of Chemical and Biomolecular Engineering.

(1) Heinrich, P.; Wyzgol, R.; Schrader, B.; Hatzilazaru, A.; Luebbers, D. W. *Appl. Spectrosc.* **1990**, *44*, 1641−1646.
(2) Krska, R.; Taga, K.; Kellner, R. *Appl. Spectrosc.* **1993**, *47*, 1484−1487.
(3) Goebel, R.; Krska, R.; Neal, S.; Kellner, R. *Fresenius' J. Anal. Chem.* **1994**, *350*, 514−519.
(4) Mizaikoff, B.; Goebel, R.; Krska, R.; Taga, K.; Kellner, R.; Tacke, M.; Katzir, A. *Sens. Actuators, B* **1995**, *B29*, 58−63.
(5) Walsh, J. E.; MacCraith, B. D.; Meaney, M.; Vos, J. G.; Regan, F.; Lancia, A.; Artjushenko, S. *Analyst (Cambridge, U.K.)* **1996**, *121*, 789−792.
(6) Jakusch, M.; Mizaikoff, B.; Kellner, R.; Katzir, A. *Sens. Actuators, B* **1997**, *B38*, 83−87.
(7) Mizaikoff, B. *Meas. Sci. Technol.* **1999**, *10*, 1185−1194.
(8) Kraft, M.; Mizaikoff, B. *Int. J. Environ. Anal. Chem.* **2000**, *78*, 367−383.
(9) Holst, G.; Mizaikoff, B. *Handbook of Optical Fibre Sensing Technology*; 2002; pp 729−755.
(10) Beyer, T.; Hahn, P.; Hartwig, S.; Konz, W.; Scharring, S.; Katzir, A.; Steiner, H.; Jakusch, M.; Kraft, M.; Mizaikoff, B. *Sens. Actuators, B* **2003**, *B90*, 319−323.
(11) Kraft, M.; Jakusch, M.; Karlowatz, M.; Katzir, A.; Mizaikoff, B. *Appl. Spectrosc.* **2003**, *57*, 591−599.
(12) Mizaikoff, B. *Anal. Chem.* **2003**, *75*, 258A−267A.
(13) Mizaikoff, B. *Water Sci. Technol.* **2003**, *47*, 35−42.
(14) Steiner, H.; Jakusch, M.; Kraft, M.; Karlowatz, M.; Baumann, T.; Niessner, R.; Konz, W.; Brandenburg, A.; Michel, K.; Boussard-Pledel, C.; Bureau, B.; Lucas, J.; Reichlin, Y.; Katzir, A.; Fleischmann, N.; Staubmann, K.; Allabashi, R.; Bayona, J. M.; Mizaikoff, B. *Appl. Spectrosc.* **2003**, *57*, 607−613.
(15) Steiner, H.; Staubmann, K.; Allabashi, R.; Fleischmann, N.; Katzir, A.; Reichlin, Y.; Mizaikoff, B. *Water Sci. Technol.* **2003**, *47*, 121−126.
(16) Karlowatz, M.; Kraft, M.; Mizaikoff, B. *Anal. Chem.* **2004**, *76*, 2643−2648.
(17) Fahrenfort, J. *Spectrochim. Acta* **1961**, *17*, 698−709.
(18) Harrick, N. J. *Internal Reflection Spectroscopy*; Harrick: Ossining, NY, 1979.
(19) Goebel, R.; Krska, R.; Kellner, R.; Seitz, R. W.; Tomellini, S. A. *Appl. Spectrosc.* **1994**, *48*, 678−683.
(20) MacCraith, B. D. *Crit. Rev. Opt. Sci. Technol.* **1997**, *CR68*, 64−89.
(21) Han, L.; Niemczyk, T. M.; Lu, Y.; Lopez, G. P. *Appl. Spectrosc.* **1998**, *52*, 119−122.
(22) Janotta, M.; Karlowatz, M.; Vogt, F.; Mizaikoff, B. *Anal. Chim. Acta* **2003**, *496*, 339−348.
(23) Janotta, M.; Katzir, A.; Mizaikoff, B. *Appl. Spectrosc.* **2003**, *57*, 823−828.

10.1021/ac070832g CCC: $37.00
Published on Web 11/17/2007

at the waveguide surface by drip-coating or spin-coating.[1,2,24] Suitable enrichment layers are generally selected by screening a wide variety of commercially available carbon-based polymers without deliberate tailoring of chemical or physical properties for targeting a specific analyte.[1,19] Alternatively, spin-coated or drip-coated sol−gel films provide mechanically robust sensing membranes with substantial chemical and physical tunability.[20−23] Surface polarity can be independently controlled by selecting appropriate termination of silicone precursors (i.e., organically modified silicones; ORMOSILs),[20,25] and the silicate matrix porosity can be modified by selecting acid- or base-catalyzed copolymerization conditions of the sol solution prior to deposition.[22,23,25] While the extended tunability of physical and chemical properties of sol−gel layers to optimize analyte sensitivity and transport is attractive, extensive preparation periods (>1 week for aging) are typically required to generate applicable membranes.[22,25] In this study, we present plasma-polymerized films as a novel, third class of enrichment membranes for liquid-phase IR-ATR sensors, which uniquely enables rapid (<3 h) preparation and deposition of widely tunable carbon-based sensing layers with scalable batch production capability. Furthermore, plasma-deposited sensing interfaces are applicable to virtually any membrane-based liquid-phase chemical sensing scheme irrespective of the underlying transduction principle (optical, electrochemical, mechanical/mass, etc.) if generation of the analytical signal requires partitioning of the target analyte(s) into a molecular recognition matrix.

Plasma polymerization is a process whereby organic gases or vapors are excited by an electric discharge and deposit as a highly cross-linked thin film grafted from an exposed surface. Plasma-generated films are a common surface modification for altering the adhesion, biocompatibility, insulation, printability, corrosive protection, and hydrophobicity of various substrates.[26−31] In addition, plasma polymer membranes can be tailored to enhance chemical and thermal stability, mechanical strength, and thickness uniformity at the nanoscale.[31−33] Among other parameters, tunability of the chemical structure and composition of plasma-deposited films can be achieved by varying process conditions including selection of the monomer(s), monomer(s) flow rate, rf power level, reactor pressure, substrate temperature, and frequency of the discharge, including continuous or pulsed mode, which provides multiple degrees of freedom conducive for application-oriented optimization of liquid-phase sensing membranes.[31]

Plasma films have been applied as molecular recognition membranes in vapor and gas-phase chemical sensing applications in combination with a variety of signal transduction principles.[34−48] The versatility of plasma-polymerized sensing layers is exemplified in the development of array-based chemical sensors utilizing quartz crystal resonators as mass-sensitive transducers coated with different plasma films serving as pattern recognition sensing elements for odor classification, air monitoring, and breath diagnostics.[37,39,43,45−47] In liquid, plasma-polymerized films have to date been applied as structural immobilization scaffolds without direct involvement in signal transduction.[49−51]

Plasma-deposited films from pentafluoroethane (PFE) vapor have been extensively investigated for their thermal stability,[52] sorption and desorption of moisture and organic vapors,[44,48] and structure−property relationships with respect to plasma chemistry.[53] In addition, plasma-polymerized PFE films exhibit only a few minor infrared absorption features between 1100 and 680 cm^{-1} thus providing an excellent monomer choice for investigating the feasibility of plasma-deposited layers as liquid-phase sensing membranes.[52,54] In this study, we demonstrate initial capabilities of a carbon-based plasma-polymerized membrane serving as an enrichment layer for liquid-phase sensors targeting trace levels of tetrachloroethylene (TeCE) in aqueous media utilizing evanescent field absorption spectroscopy as an exemplary signal transduction scheme. Additionally, we provide a tabular review facilitating a comparison of typical figures of merit reported for various IR-ATR polymer/waveguide combinations for trace detection of TeCE since the pioneering work of Heinrich et al. in 1990.[1]

(24) Murphy, B.; McLoughlin, P. *Int. J. Environ. Anal. Chem.* **2003**, *83*, 653−662.
(25) Han, L.; Niemczyk, T. M.; Haaland, D. M.; Lopez, G. P. *Appl. Spectrosc.* **1999**, *53*, 381−389.
(26) Brewis, D. M.; Briggs, D. *Polymer* **1981**, *22*, 7−16.
(27) Biederman, H.; Osada, Y. *Plasma Polymerization Processes*; Elsevier Science Publishing Company Inc.: New York, 1992.
(28) Hopkins, J.; Wheale, S. H.; Badyal, J. P. S. *J. Phys. Chem.* **1996**, *100*, 14062−14066.
(29) Wang, T. F.; Lin, T. J.; Yang, D. J.; Antonelli, J. A.; Yasuda, H. K. *Prog. Org. Coat.* **1996**, *28*, 291−297.
(30) Yasuda, H. K.; Wang, T. F.; Cho, D. L.; Lin, T. J.; Antonelli, J. A. *Prog. Org. Coat.* **1997**, *30*, 31−37.
(31) Biederman, H. *Plasma Polymer Films*; Imperial College Press: London, 2004.
(32) Sahin, H. T.; Manolache, S.; Young, R. A.; Denes, F. *Cellulose (Dordrecht, Neth.)* **2002**, *9*, 171−181.
(33) Mukhopadhyay, S. M.; Joshi, P.; Datta, S.; Zhao, J. G.; France, P. *J. Phys. D: Appl. Phys.* **2002**, *35*, 1927−1933.
(34) Inagaki, N.; Ohkubo, J. *J. Appl. Polym. Sci.* **1991**, *43*, 793−800.
(35) Sugimoto, I. *J. Appl. Phys.* **1991**, *70*, 2887−2889.
(36) Sugimoto, I.; Nakamura, M.; Kuwano, H. *Sens. Actuators, B* **1993**, *B10*, 117−122.
(37) Nakamura, M.; Sugimoto, I.; Kuwano, H.; Lemos, R. *Sens. Actuators, B* **1994**, *20*, 231−237.
(38) Guo, S.; Rochotzki, R.; Lundstrom, I.; Arwin, H. *Sens. Actuators, B* **1997**, *B44*, 243−247.
(39) Kasai, N.; Sugimoto, I.; Nakamura, M.; Katoh, T. *Biosens. Bioelectron.* **1999**, *14*, 533−539.
(40) Partridge, A.; Harris, P.; Hirotsu, T.; Kurosawa, S. *Plasmas Polym.* **2000**, *5*, 191−200.
(41) Nanto, H.; Hamaguchi, Y.; Sanada, S.; Nobuyama, K.; Matsumoto, T.; Tanabe, K.; Kurosawa, S. *Chem. Sens.* **2001**, *17*, 363−365.
(42) Avramov, I. D.; Rapp, M.; Kurosawa, S.; Krawczak, P.; Radeva, E. I. *IEEE Sens. J.* **2002**, *2*, 150−159.
(43) Seyama, M.; Sugimoto, I.; Miyagi, T. *IEEE Sens. J.* **2002**, *2*, 422−427.
(44) Tanikella, R. V.; Agraharam, S.; Bidstrup Allen, S. A.; Hess, D. W.; Kohl, P. A. *J. Electron. Mater.* **2002**, *31*, 1096−1103.
(45) Seyama, M.; Iwasaki, Y.; Sugimoto, I.; Tate, A.; Niwa, O. *Chem. Sens.* **2004**, *20*, 256−257.
(46) Seyama, M.; Sugimoto, I.; Nakamura, M. *Biosens. Bioelectron.* **2004**, *20*, 814−824.
(47) Nanto, H.; Kitade, Y.; Sekikawa, Y.; Takei, Y.; Kubota, N.; Kusano, E.; Kinbara, A. *Proc. SPIEsInt. Soc. Opt. Eng.* **2004**, *5270*, 174−181.
(48) Vaswani, S.; Koskinen, J.; Hess, D. W. *J. Vac. Sci. Technol., A* **2006**, *24*, 1737−1745.
(49) Yoshimura, K.; Hozumi, K. *Microchem. J.* **1996**, *53*, 404−412.
(50) Yoshimura, K.; Hozumi, K. *Microchem. J.* **1996**, *53*, 207−214.
(51) Zhang, Z.; Knoll, W.; Foerch, R. *Surf. Coat. Technol.* **2005**, *200*, 993−995.
(52) Agraharam, S.; Hess, D. W.; Kohl, P. A.; Bidstrup Allen, S. A. *J. Electrochem. Soc.* **2000**, *147*, 2665−2670.
(53) Agraharam, S.; Hess, D. W.; Kohl, P. A.; Bidstrup Allen, S. A. *J. Vac. Sci. Technol., B: Microelectron. Nanometer Struct.—Process., Meas., Phenom.* **2001**, *19*, 439−446.
(54) Agraharam, S.; Hess, D. W.; Kohl, P. A.; Bidstrup Allen, S. A. *J. Vac. Sci. Technol., A* **1999**, *17*, 3265−3271.

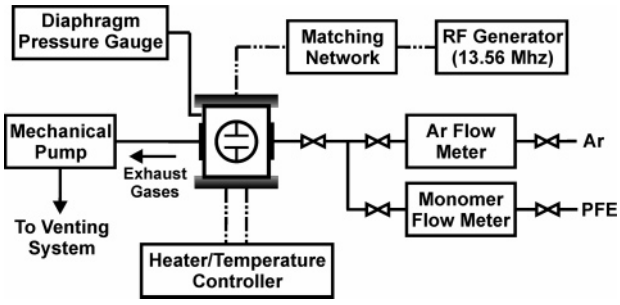

Figure 1. Diagram of 6 in. parallel plate plasma reactor setup for plasma-assisted deposition of PFE films onto ZnSe substrates.

EXPERIMENTAL SECTION

Plasma Reactor Reagents. Pentafluoroethane monomer gas (N4 grade, 99.99%) and argon carrier gas (ultrahigh purity, 99.99%) were purchased from Jackson Laboratory (Deepwater, NJ) and Chemicals Inc. (Allentown, PA), respectively. Oxygen (ultrapure carrier, 99.996%) and nitrogen (ultrahigh purity, 99.999%) were purchased from Airgas Inc. (Radnor, PA).

IR-ATR Reagents. Tetrachloroethylene (99.9+%, HPLC grade) was purchased from Sigma-Aldrich (St. Louis, MO). TeCE is a toxic chemical and should only be handled with appropriate gloves such as polyvinyl alcohol under a fume hood. Deionized water (R = 18.2 MΩ·cm at 25 °C) was used for preparation of all TeCE solutions and for equilibration/regeneration of the sensing membranes.

Plasma Deposition of PFE Films. A 6 in. parallel plate plasma reactor (see Figure 1) was used to deposit PFE films (n_D approximately 1.41−1.42 at 632.8 nm)[53] at a temperature and pressure of 110 °C and 1 torr, respectively. The bottom electrode was grounded and heated to 110 °C using Omegalux CIR 2015 cartridge heaters (Omega Engineering Inc., Stamford, CT). The temperature at the bottom electrode was monitored using a type K thermocouple controlled by a Syskon RKC temperature controller (RKC Instrument Inc., Southbend, IN). The top electrode of the reactor was connected to an HF-300 13.56 MHz, 120 W rf power supply (ENI Power Systems, Rochester, NY). A matching network (Heathkit SA-2060A, Heath Company, Benton Harbor, MI) was connected between the top electrode and the power supply to minimize reflected power in the plasma reactor. The reactor pressure was monitored and maintained at 1 torr using a pressure gauge (Varian Inc., Lexington, MA) and an Alcatel 2063 C rotary vacuum pump (Alcatel, Annecy, France).

The plasma reactor is continuously maintained at a base pressure of 0.02 torr during nonoperational periods. Prior to loading ZnSe waveguides as the target substrates, the bottom electrode was heated to 110 °C, and the reactor was vented to atmospheric pressure with nitrogen gas. The reactor was sealed and evacuated to a base pressure of 1 torr after sample placement. ZnSe waveguides were first exposed to an oxygen plasma (O_2 gas at a flow rate of 75 standard cm^3/min) to oxidize and remove organic residue from the target surface. PFE monomer and argon gas were then introduced at a flow rate of 20 and 75 standard cubic centimeters/min, respectively. Finally, the rf generator was activated for film deposition after stabilization of the reactor pressure and temperature.

Film Thickness Determination with Atomic Force Microscopy. Atomic force microscopy (AFM) experiments were performed to determine the film thickness of the deposited PFE layers. All measurements were obtained with a PicoPlus/4500 atomic force microscope (Agilent Technologies, Tempe, AZ) equipped with a large-range multipurpose scanner (maximum scan range: 100 μm × 100 μm in air). Prior to thickness determination, part of the PFE film was gently removed to expose a small section of ZnSe crystal using a razor blade and a cotton applicator. Imaging was performed in contact mode using silicon nitride cantilevers (length, 200 μm; nominal spring constant, 0.06 N m^{-1}) with integrated pyramidal tips (base, 4 μm × 4 μm; height, 2.86 μm). The imaging rate was 1.1 Hz.

IR-ATR Measurements. Fourier transform infrared (FT-IR) ATR spectra were recorded in a spectral range of 4000−400 cm^{-1} using a Bruker Equinox 55 FT-IR spectrometer (Bruker Optics Inc., Billerica, MA) equipped with a liquid nitrogen cooled mercury−cadmium−telluride (MCT) detector (Infrared Associates, Stuart, FL) and Specac Gateway in-compartment horizontal ATR unit (Specac Inc., Woodstock, GA). Trapezoidal ZnSe (n_D = 2.43 at λ = 5 μm) ATR crystals (MacroOptica, Moscow, Russia) with six effective reflection regions (72 mm × 10 mm × 6 mm; 45 °) were mounted in a customized stainless steel flow cell (2 mL volume; exposed crystal surface area approximately 7.2 cm^2). IR-ATR spectra of PFE films, TeCE enrichment, and sensor regeneration were generated by averaging 100 scans at a spectral resolution of 4 cm^{-1} over a period of approximately 25 s.

Prior to IR-ATR measurements, minor film deposits at the unprotected waveguide coupling facets were removed using a cotton applicator lightly swabbed with acetone. Plasma-deposited films were then equilibrated with deionized water for at least 18 h prior to enrichment studies. Sample solutions were individually prepared immediately prior to analysis by solvating known volumes of TeCE from a 0.5−10 μL Eppendorf pipet (calibrated pipet with error <0.3% RSD by volume; Eppendorf North America Inc., New York, NY) in degassed deionized water. An AliTea C8-MIDI peristaltic pump (Watson Marlow Alitea, Wilmington, MA) was used to pull solutions through the flow cell at a rate of 5.1 ± 0.2 mL/min. Stainless steel tubing ($^1/_{16}$ in. o.d.) was utilized to minimize analyte loss during solution transport.

Two sets of measurements (batch 1 and batch 2) were used to generate calibration curves to assess the enrichment characteristics of plasma-deposited films. TeCE concentrations ranging from 500 to 10 000 ppb (v/v) were consecutively evaluated from low to high concentrations using a spectrum of the water-equilibrated PFE layer as a reference. Once measurements encompassing the full concentration range were completed, the sensing layer was regenerated with deionized water until no detectable TeCE absorption features were evident. Thereafter, a new reference spectrum was collected and the procedure repeated. IR-ATR spectra were collected at 60 s intervals during enrichment and 120 s intervals during regeneration of the membrane.

RESULTS

IR Absorption Characteristics of PFE Films. FT-IR measurements for the spectroscopic characterization of plasma-polymerized PFE films have previously been reported.[52,54] PFE layers exhibit characteristic absorption features resulting from C−F$_x$ stretching vibrations at 1400−1000 cm^{-1}, with additional minor bands derived from C−H and C=C bonds throughout the mid-infrared regime (2−20 μm). The IR-ATR single-beam trans-

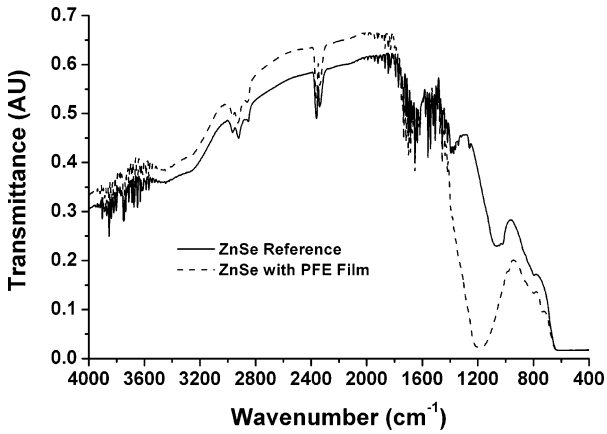

Figure 2. IR-ATR transmittance profiles for a bare ZnSe waveguide and a 700 nm plasma-polymerized PFE-coated ZnSe waveguide. $C-F_x$ stretching features are observed from 1400 to 1000 cm^{-1} with a wide spectral window in the fingerprint region from 1100 to 680 cm^{-1} amenable to VOC analysis.

mission profile of PFE-coated ZnSe waveguides reveals a wide spectral window in the fingerprint region (1100−680 cm^{-1}) conducive for interrogating various infrared absorption bands characteristic of VOCs as they partition into the PFE membrane (Figure 2). Additionally, excellent optical transmission through the ATR waveguide following plasma-assisted deposition corroborates the compatibility of ZnSe substrates with this coating technique.

Partitioning of Water into PFE Membranes. Although PFE films display hydrophobic properties, the fluorocarbon matrix is still subject to a small amount of water partitioning into the membrane matrix. Thus, equilibration of PFE layers with deionized water minimizes baseline drifts resulting from water sorption and resultant membrane swelling during quantitative measurements. Eighteen hours of conditioning provided sufficient background stabilization for subsequent evaluation of analytes dissolved in aqueous matrices.

In addition to the primary purpose of serving as an enrichment membrane for TeCE, PFE membranes concurrently suppress spectral interferences from water. Both tasks are most effectively achieved if the membrane thickness extends beyond the area actively probed by the exponentially decaying evanescent field. The penetration depth (d_p) of the evanescent field (approximately 1.2 μm at 900 cm^{-1} for the present ATR configuration) in this study extends beyond the film thickness (approximately 700 nm ± 40 nm) at wavenumbers <1400 cm^{-1}. When evaluating the C−Cl absorption band at 913 cm^{-1} for quantitative analysis of TeCE, water interference is of minor concern; hence, the current configuration enables the establishment of a first sensitivity benchmark for IR chemical sensing with plasma-deposited membranes for future optimization. Consequently, extension of the film thickness beyond the penetration depth of the evanescent field in future studies can facilitate spectral access to additional target analyte absorption features, improved signal-to-noise ratio, and reduced detection limits; however, an increased film thickness affects efficient analyte transport to the sensing interface for diffusion-based sensors.

TeCE Enrichment Characteristics. Tetrachloroethylene exhibits a variety of spectral features in the fingerprint region (1300−500 cm^{-1}). For this study, peak integration (i.e., integrated peak area (AU/cm)) of the strongest TeCE absorption feature, the ν(C−Cl) mode at 913 cm^{-1}, was evaluated for quantitative analysis. Figure 3A displays the reproducible dynamic response of the IR-ATR sensor obtained for triplicate measurements comprising five individually prepared aqueous TeCE concentrations along with appropriate sensing layer regeneration steps. Figure 3B provides an accentuated view of the integrated peak area response for a selected concentration level illustrating signal stabilization in response to analyte exposure. In addition, representative TeCE infrared signatures for the five analyzed concentrations are shown in Figure 3C.

TeCE partitioning reaches equilibrium after approximately 35 min at 500 ppb (v/v) concentrations, with acceptable T_{90} (time required for 90% of full signal) times at approximately 30 min. The reported T_{90} values for TeCE enrichment into the PFE layers are approximately twice the reported values for comparable IR-ATR measurements with Teflon AF 1600 (16.6 min) and Teflon AF 2400 (13.6 min) membranes.[24,55,56] This is expected, since plasma-polymerized PFE membranes represent highly cross-linked networks of monomer units, which is different from typical spin-coated membranes reconstituted from solvated polymer solutions. Complete regeneration of the enrichment membrane following the evaluation of 10 ppm (v/v) TeCE solutions was achieved after approximately 95 min by flushing with deionized water at 5.1 mL/min.

For measurements at 500 ppb (v/v), the diffusion rate for TeCE into a 700 nm PFE layer was calculated to be on the order of 2×10^{-12} cm^2/s using the approach presented by Fieldson and Barbarie.[57] The calculated diffusion rate for TeCE into PFE films is considerably lower than reported diffusion rates of TeCE into Teflon AF2400 membranes of 3.18×10^{-10} cm^2/s,[24] which is consistent with the observed TeCE equilibration times reported in this study. The extended duration of analyte transport is attributed to smaller void volumes in the fluorocarbon network resulting from the high degree of monomer cross-linking obtained during plasma deposition of PFE films.

Despite comparatively slower analyte transport into PFE membranes, limits of detection (LOD) below 300 ppb (v/v) for TeCE were obtained from two separate batches of plasma-deposited films (LOD definition: 3σ; concentration determination from the regression fit using the criterion of 3 times the noise of a blank sample). Figure 4 provides calibration curves based on integrated peak areas for TeCE enriched into plasma-deposited PFE membranes. Batch 1 (thickness undetermined) indicates the initial calibration series utilized to establish the feasibility and behavior of a dose-dependent response to TeCE. Initially, four concentrations in the range of 500−10 000 ppb (v/v) were analyzed in triplicate with error bars representing the calculated standard deviation. Departure from a first-order linear response was confirmed during an extended evaluation of five TeCE solutions over the same concentration range with a batch 2 waveguide. TeCE LODs were calculated for batch 1 and batch 2 as 265 and 299 ppb (v/v), respectively. Higher signal strength

(55) McLoughlin, P.; Flavin, K.; Kirwan, P.; Murphy, B.; Murphy, K. *Sens. Actuators, B* **2005**, *B107*, 170−177.
(56) Murphy, B.; Kirwan, P.; McLoughlin, P. *Anal. Bioanal. Chem.* **2003**, *377*, 195−202.
(57) Fieldson, G. T.; Barbari, T. A. *AIChE J.* **1995**, *41*, 795−804.

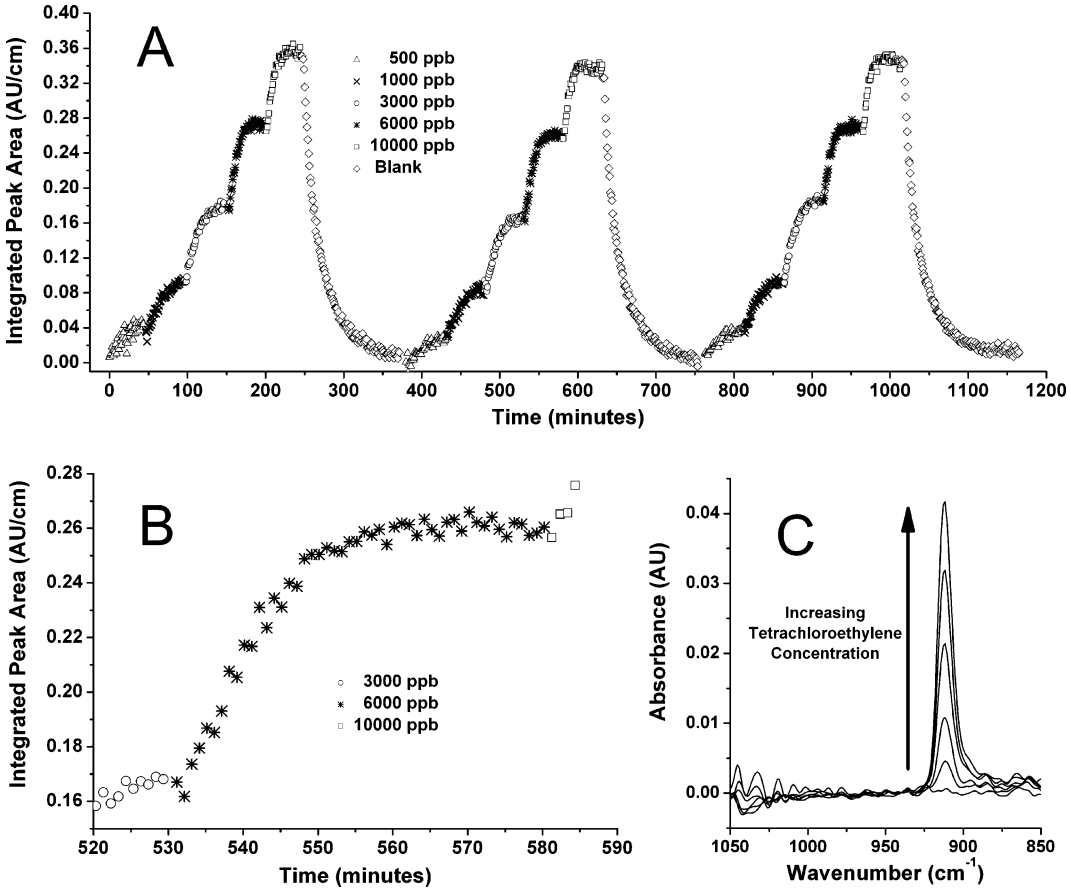

Figure 3. IR-ATR experimental results displaying (A) the dynamic response for five TeCE concentrations increasing from 500 to 10 000 ppb (v/v) and sensor regeneration with deionized water, (B) an accentuated view of IR-ATR sensor response for a single TeCE concentration displaying analyte equilibration and signal stability, and (C) representative IR-ATR signatures of TeCE for the ν(C−Cl) stretching vibration at approximately 913 cm^{-1} for the five examined TeCE concentrations (500, 1000, 3000, 6000, and 10 000 ppb, v/v) and a blank sample (batch 2 of PFE-coated waveguides).

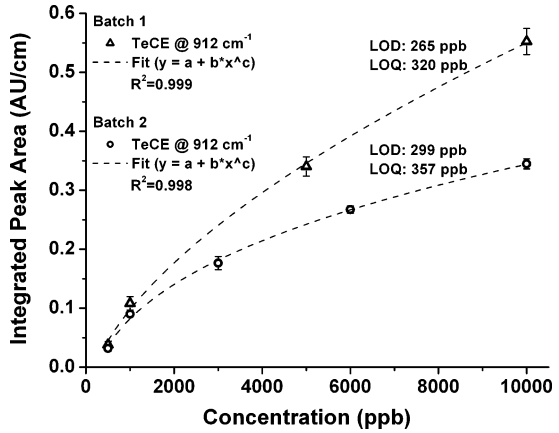

Figure 4. Calibration for TeCE in the range of 500−10 000 ppb (v/v) utilizing integrated peak area analysis. Error bars represent one standard deviation for three repeated measurements. Limit of detection (LOD, 3σ) and limit of quantification (LOQ, 6σ) are provided in addition to the fit equation and goodness of the fit. χ^2 tests evaluating the goodness of fit for each calibration trial provided $P < 0.001$; $P = 0.00004$, and $P = 0.0002$ for batch 1 and batch 2, respectively. For batch 1 $A = -0.0589$, $B = 0.0027$, and $C = 0.5895$. For batch 2 $A = -0.1324$, $B = 0.0196$, and $C = 0.3465$.

and improved sensitivity obtained from a batch 1 waveguide indicates the deposition of a thicker film compared to batch 2 (700 nm) and illustrates the potential for improved sensor response by tailoring the deposition conditions and duration for generating thicker films on ZnSe substrates.

Although sub-d_p film thicknesses were utilized in this first feasibility study, the calculated LODs below 300 ppb (v/v) for TeCE already compare favorably to the reported detection limits in literature ranging from 20 ppb to approximately 2 ppm (v/v) for various IR-ATR sensing schemes with different polymer/waveguide combinations (Table 1).[1,2,6,10,11,19,24,55,56,58−60] Although reduced response times were observed; it is anticipated that improved LODs will be obtained by enhanced analyte transport characteristics upon future tailoring of the cross-link density and film thickness.

Lifetime of the PFE Membrane. Currently, plasma-deposited PFE layers on ZnSe surfaces withstand approximately 4−5 days of continuous flow exposure before degradation occurs due to patchy film delamination from the substrate surface, currently limiting long-term applications. PFE detachment is likely resulting from swelling-induced interfacial stress that correlates with the cross-link density of plasma-polymerized films, i.e., higher cross-

(58) Goebel, R.; Krska, R.; Kellner, R.; Katzir, A. *Fresenius' J. Anal. Chem.* **1994**, *348*, 780−781.
(59) Michel, K.; Bureau, B.; Boussard-Pledel, C.; Jouan, T.; Adam, J. L.; Staubmann, K.; Baumann, T. *Sens. Actuators, B* **2004**, *B101*, 252−259.
(60) Roy, G.; Mielczarski, J. A. *Water Res.* **2002**, *36*, 1902−1908.

Table 1. Survey of Reported LODs for Tetrachloroethylene (TeCE) Utilizing Various Combinations of IR-ATR Sensing Platforms and Enrichment Membranes, Including Field Deployable Systems

ref no.	ATR configuration	enrichment membrane	thickness	LOD (v/v)	T_{90} (min)
this study	trapezoidal (6 reflections)	plasma-deposited PFE	700 nm	265 ppb	5
1	trapezoidal (7 reflections)	poly(ether-esteramide)	5−20 μm	616 ppb	100
1	trapezoidal (7 reflections)	polyethylene (ρ = 0.96 g/cm^3)	5−20 μm	1.54 ppm	6
1	trapezoidal (7 reflections)	polyethylene (ρ = 0.937 g/cm^3)	5−20 μm	185 ppb	12
1	trapezoidal (7 reflections)	polyethylene (ρ = 0.89 g/cm^3)	5−20 μm	123 ppb	
1	trapezoidal (7 reflections)	trichloroctadecylsilane	5−20 μm	308 ppb	0.4−1.4
2	37 cm silver halide fiber (1 mm dia., 10 cm active length)	low-density polyethylene	15−17 μm	616 ppb	∼15
19	trapezoidal (8 reflections)	polyisobutylene	20−24 μm	1.23 ppm	35
6	U-shaped silver halide fiber (0.7 mm dia., unspecified active length)	poly(ethylene-*co*-propylene)	10 μm	300 ppb	18
60	trapezoidal (8 reflections)	poly(ethylene-*co*-propylene)	1 μm	19.6 ppb	∼7
24	trapezoidal (6 reflections)	Teflon AF 1600 and 2400	6.8 μm, 5.3 μm	low ppm[a]	16.6, 13.6[b]
11	U-shaped silver halide fiber (0.7 mm dia., 38 cm active length)	poly(ethylene-*co*-propylene)	6 μm	20 ppb	<10
10	straight silver halide fiber (unspecified active length)	poly(ethylene-*co*-propylene)	25−30 μm	900 ppb (6σ)	5
59	20 cm tapered chalcogenide fiber (100 μm thickness)	none	N/A	616 ppb	N/A
58	straight silver halide fiber (1 mm dia., 16 cm active length	polyisobutylene	14 μm	616 ppb	∼15

[a] Detection limit for TeCE not explicitly specified. [b] Sensing times of approximately 15 min have also been reported for Teflon AF 2400 in Murphy et al. and McLoughlin et al. (refs 55 and 56).

link densities induce enhanced interfacial stress.[61] Hence, the sensing platform operational lifetime can potentially be extended by adjusting the cross-link density of the fluorocarbon matrix to reduce interfacial stress, while concurrently improving analyte transport properties. This will be the subject of future studies.

CONCLUSIONS

We have demonstrated the first liquid-phase sensing application of plasma-deposited thin films serving as an enrichment membrane in combination with IR-ATR evanescent field absorption sensors targeting trace detection of VOCs in aqueous environments. Benchmark characteristics for sensitivity, reproducibility, and enrichment behavior of plasma-polymerized PFE films have been established for a model analyte (TeCE) providing competitive results in comparison to already established IR-ATR membrane configurations, yet offering substantial potential for deliberate manipulation of the physical and molecular recognition properties of the sensing membrane. In addition, plasma-polymerized films offer unsurpassed chemical and mechanical stability at temperatures exceeding 300 °C, which renders them ideal materials for diffusion-based chemical sensing applications in harsh environmental and industrial settings. Consequently, this well-developed coating strategy exhibits the required flexibility and tunability to assist the development of next-generation liquid-phase sensing membranes applicable at extreme conditions, while providing scalable batch production capabilities.

(61) Igarashi, S.; Itakura, A. N.; Toda, M.; Kitajima, M.; Chu, L.; Chifen, A. N.; Foerch, R.; Berger, R. *Sens. Actuators, B* **2006**, *B117*, 43−49.

ACKNOWLEDGMENT

The authors thank Dr. Prabhaker Tamirisa and Dr. Nicola Menegazzo for their assistance throughout this project.

Received for review April 24, 2007. Accepted September 11, 2007.

AC070832G